Integrating spatial capture-recapture models with variable individual identifiability

JOEL S. RUPRECHT[1,*], CHARLOTTE E. ERIKSSON[1], TAVIS D. FORRESTER[2], DARREN A. CLARK[2], MICHAEL J. WISDOM[3], MARY M. ROWLAND[3], BRUCE K. JOHNSON[2,†], AND TAAL LEVI[1]

[1]*Department of Fish and Wildlife, 104 Nash Hall, Oregon State University, Corvallis, OR 97331*

[2]*Oregon Department of Fish and Wildlife, 1401 Gekeler Lane, La Grande, OR 97850*

[3]*Pacific Northwest Research Station, USDA Forest Service, 1401 Gekeler Lane, La Grande, OR 97850*

†Retired

**Email: joel.ruprecht@oregonstate.edu*

Abstract. Many applications in ecology depend on unbiased and precise estimates of animal population density. Spatial capture recapture models and their variants have become the preferred tool for estimating densities of carnivores. Within the spatial capture-recapture family are variants that require individual identification of all encounters (spatial capture-recapture), individual identification of a subset of a population (spatial mark-resight), or no individual identification (spatial count). In addition, these models can incorporate telemetry data (all models) and the marking process (spatial mark-resight). However, the consistency of results

among methods and the relative precision of estimates in a real-world setting are unknown. Consequently, it is unclear how much and what type of data are needed to achieve satisfactory density estimates. We tested a suite of models to estimate population densities of black bears (*Ursus americanus*), bobcats (*Lynx rufus*), cougars (*Puma concolor*), and coyotes (*Canis latrans*). For each species we genotyped fecal DNA collected with detection dogs. A subset of individuals from each species were affixed with GPS collars bearing unique markings to be resighted by remote cameras set on a 1 km grid. We fit 10 models for each species ranging from those requiring no animals to be individually recognizable to others that necessitate full individual recognition. We then assessed the contribution of incorporating telemetry data to each model and the marking process to the mark-resight model. Finally, we developed an integrated hybrid model that combines camera, physical capture, genetic, and GPS data into a single hierarchical model. Importantly, we find that spatial count models that do not individually identify animals fail in all cases whether or not telemetry data are included. Results improved as models contained more information on individual identity. Models where a subset of individuals were identifiable yielded qualitatively similar results, but can produce quantitatively divergent estimates, suggesting that long-term population monitoring should use a consistent method across years. Incorporation of telemetry data and the marking process can produce more accurate and precise density estimates. Our results can be used to guide future study designs to efficiently estimate carnivore densities for better understanding of population dynamics, predator-prey relationships, and community assemblages.

Key words: abundance, black bear, bobcat, camera trapping, carnivore, count, cougar, coyote, density estimation, mark resight, noninvasive genetic sampling, spatial capture recapture

INTRODUCTION

Population abundance is a state variable of paramount importance in both applied and basic ecology but remains a challenge to estimate for most free-ranging animal populations. This is particularly the case for terrestrial carnivore species that are cryptic and occur at low densities, which preclude observational censuses or sightability-corrected survey methods (Wilson and Delahay 2001). Many statistical models accounting for imperfect detection have been used to estimate abundance, but the data required for each method vary along a continuum of recognition of individual animals, ranging from no individual recognition to full individual recognition. For data-poor situations in which no animals can be uniquely identified, models to estimate abundance have been developed based on presence-absence of unmarked individuals in a sampling session (Royle and Nichols 2003) or counts of unmarked individuals (Buckland et al. 1993, Royle 2004, Rowcliffe et al. 2008, Chandler and Royle 2013, Moeller et al. 2018). Other models rely on partially-observable encounter histories when a subset of the population is identifiable (e.g. White 1996, McClintock and White 2009, Sollmann et al. 2013a, Augustine et al. 2018), and data-rich models utilize fully-observable encounter histories such that all individuals can be uniquely identified (e.g., Otis et al. 1978, Nichols 1992, Royle et al. 2013). Collecting higher resolution data where individuals are identifiable is substantially more challenging, but models based on these data may produce more robust estimates of abundance, particularly when the more demanding assumptions for data-poor models are violated (Chandler and Royle 2013, Augustine et al. 2019). Knowing what type and how much data to collect to achieve unbiased results with satisfactory precision, yet not beyond that required, is therefore a central challenge to estimate population abundance for conservation, management, or research objectives.

Spatial capture recapture (SCR; Borchers and Efford 2008, Royle and Young 2008) has emerged as the most prominent method of abundance estimation for carnivores over the past five years (Appendix S1: Fig. S1). SCR models exploit the spatial locations of animal detections and assume the rate or probability an individual is detected is highest at its home range center and declines as distance from the home range center increases (Royle and Young 2008). The spatially-referenced detections of an individual allow the estimation of the animal's activity center, and the number of estimated activity centers yields an estimate of abundance. Population density, often preferable to abundance, is calculated by dividing the estimated number of activity centers by the area of the state space, which eliminates the arbitrarily defined effective sampling area required in traditional capture-mark-recapture approaches (Royle et al. 2013). Furthermore, SCR can accommodate individual and trap-level covariates to explain spatial and individual variation in detection rates.

SCR models are well-suited for noninvasive genetic sampling in which individuals are uniquely identified, typically using DNA from feces or hair samples, to produce fully-observable encounter histories (Gardner et al. 2009, Kery et al. 2011, Morin et al. 2016, 2018). Scat-detection dogs in particular have become a common tool to efficiently collect feces on large landscapes within a narrow time window to ensure demographic closure even for species that occur at low densities (Wasser et al. 2004, 2011). While effective for SCR density estimation, scat detection requires highly-trained dogs and specialization in genetic techniques or the resources to contract out those tasks. As a more inexpensive and accessible alternative, wildlife researchers increasingly use remote cameras to study and monitor wildlife. However, cameras can only be used for conventional SCR analyses when all individuals of a species possess natural

91 markings (e.g. unique pelage patterns) that permit individual identification (but see Augustine et
92 al. 2018).

93 Spatial mark-resight (SMR) and generalized spatial mark-resight (gSMR) models are
94 variants of SCR that allow spatially-explicit density estimation when only a subset of the
95 population can be uniquely identified (Chandler and Royle 2013, Sollmann et al. 2013a,
96 Whittington et al. 2018). A common example is identification of individual study animals that
97 are collared (i.e., marked) from a population of interest. For many species it would be inefficient
98 to capture and mark animals solely for the purpose of density estimation; however, many
99 researchers and wildlife management agencies routinely monitor populations with telemetry
100 devices. In these cases, resighting marked animals on an array of remote cameras may offer a
101 relatively straightforward option for estimating density at little extra cost (Whittington et al.
102 2018).

103 Due to the challenge of individually marking animals, spatial count (SC) or 'unmarked
104 SCR' models (Chandler and Royle 2013) have been developed to exploit spatial autocorrelation
105 in counts of unmarked animals to make inference on their activity centers, and by extension,
106 population density. The attractiveness of this approach is that it requires no individual
107 identification so the population need not be artificially nor naturally marked. The only data
108 required for SC models are spatially-referenced counts of animal detections, which allows use of
109 standard camera trapping datasets that can be collected noninvasively without the cost and
110 specialized equipment needed for genotyping. Should SC models produce robust density
111 estimates as suggested by Chandler and Royle (2013) and Evans and Rittenhouse (2018), they
112 would represent a major advance in our ability to rapidly and affordably count carnivores.

These three model types require data of vastly different levels of individual identifiability which raise concerns over the level of agreement in accuracy and precision with each technique. Understanding the relative performance of these commonly-used density estimators is critical to guide future population monitoring for conservation and management. We believe, *a priori*, that genetic SCR methods yield the most robust density estimates because they have the strictest data requirements in terms of individual identification. As the use of SMR and SC methods proliferates in the literature, however, it is important to evaluate their credibility with respect to the 'gold standard' SCR approach. A variety of additional data sources can be incorporated into these models, which could potentially increase the concordance of results from data poor SC models and data rich SCR models while also increasing precision and accuracy. For example, all of these models can be informed by telemetry data (Sollmann et al. 2013a) to provide independent estimates of home range size and location, and the SMR model can additionally be informed by the capture-mark-recapture process used to mark animals (Whittington et al. 2018). Since research projects and monitoring programs have limited budgets, it is also critical to know how much and what type of data must be collected to achieve unbiased results with satisfactory precision.

Here we use a unique dataset consisting of 1) genotyped scats located by detection dogs, 2) images of both marked and unmarked animals from an array of remote cameras, 3) encounter histories of physical captures to mark animals, and 4) GPS (Global Positioning System) collar locations to estimate the abundances of four carnivore species: black bears (*Ursus americanus*), bobcats (*Lynx rufus*), cougars (*Puma* concolor), and coyotes (*Canis latrans)*. Our objective is to evaluate a suite of existing spatial density models across a spectrum of data richness to evaluate agreement in results and precision. In addition, we develop a new hybrid model that can

incorporate SCR and SMR data sources (i.e. including genotypes, the physical marking process, camera data, and GPS data) into a single hierarchical model, and assess the resulting gains in precision. Notably our model comparisons occur in the context of a real system rather than simulation. Each species varies in its life history, from highly territorial but group living (coyotes), to non-territorial solitary individuals (black bears), to solitary territorial individuals with territory size varying by sex (bobcat females are territorial while males are not; cougar males are territorial while females are not). By evaluating a suite of methods with different data requirements, our findings directly address how population densities of terrestrial carnivores can most efficiently be estimated, and whether the investment in genotyping or marking and resighting animals is necessary given the availability of models that do not rely on individual identification.

METHODS

Study Area

Our study was conducted in and adjacent to the Starkey Experimental Forest and Range (hereafter Starkey) in the Blue Mountains of northeastern Oregon (Fig. 1). Starkey is bounded by a 2.4-meter fence, enclosing 100.7 km^2, which prevents the passage of large herbivores (Rowland et al. 1997); however, carnivores are undeterred by the fence and regularly cross in and out of the enclosure (this study, Oregon Department of Fish and Wildlife, unpublished data). Starkey is part of the Wallowa-Whitman National Forest and is administered by the US Forest Service. Land immediately adjacent to Starkey is predominantly public and managed by the US Forest Service (Wallowa-Whitman and Umatilla National Forests) but also includes private inholdings. The study area contains a mosaic of Ponderosa pine (*Pinus ponderosa*) stands and

mixed pine-fir forests (*Pinus*, *Abies* and *Pseudotsuga* spp.), interspersed with grasslands dominated by native bunchgrasses (*Poa*, *Danthonia*, and *Pseudoroegneria* spp.) and invasive annual grasses (*Bromus* and *Ventenata* spp.) (Rowland et al. 1997). Elevation ranges between 1,122 and 1,500 m within Starkey (Rowland et al. 1997). See Wisdom et al. (2005) for additional details about Starkey.

Data collection

Scat dataset

Scat detection dogs from the University of Washington Conservation Canine program surveyed a 224 km^2 study area encompassing all of Starkey and roughly an equal area immediately to the north and west of the enclosure between 6 and 26 June 2017 (Fig. 1). The area surveyed was composed of 56 gridcells each with an area of 4 km^2. Detection dogs surveyed 6–8 km linear distance within each cell to distribute effort across the study area. Dog handlers were not given specific survey routes but were encouraged to follow natural travel corridors such as ridgelines, saddles, drainage bottoms, game trails, and fencelines. No more than 50% of the distance traveled per gridcell was permitted to be on linear features such as trails or roads. When scats were located, the handler recorded the GPS position and placed the entire scat in triplicate paper bags. Within 72 hours of collection, scats were desiccated in a drying oven for 24 hours at 40°C (Murphy et al. 2000). Detection dogs in our study were trained to locate black bear, coyote, cougar, and bobcat scats (Fig. 2c).

We used genotyping by amplicon sequencing (Eriksson et al. 2020) to identify unique individuals with single-nucleotide polymorphisms (SNPs). Genotyping by amplicon sequencing uses the power of high-throughput sequencers to yield high genotype success rates and low error

rates. Coyote scats were genotyped following methods in Eriksson et al. (2020). We genotyped bobcat, cougar, and black bears feces using the same approach but with novel primers designed and tested specifically for this study (Appendix S2). Prior to genotyping, the identity of the defecator for each scat was identified using DNA metabarcoding of ~100bp of the mtDNA 12S region as part of a separate diet study (primers used in Eriksson et al. 2020, Massey et al. 2020, and modified from Riaz et al. 2011). See Appendix S2 for single-nucleotide polymorphism discovery methods and Eriksson et al. (2020) for detailed genotyping protocol.

Camera dataset

A 1- x 1-km grid of 94 unbaited remote cameras (Bushnell TrophyCam Aggressor, Overland, KS) was placed inside the Starkey fence perimeter and was operational between April and September 2017 (Fig. 1). All cameras were pointed north. We visited each camera station every 6-8 weeks to change batteries and download data. Each camera was set to take a burst of 3 photos when triggered.

Photos were tagged to species or to individual when animals were uniquely identifiable due to GPS collars and ear tags. We used the open source photo management software DigiKam (www.digikam.org) for tagging and database management and the R library camtrapR (Niedballa et al. 2016) to extract metadata from photos. We censored photos in which we could not determine whether an animal was wearing a GPS collar or if we could not verify the identity of an animal photographed with a GPS collar. However, these records constituted < 5% of all detections. Because animals were typically photographed more than once during a visit, we recorded information for each independent photo sequence and considered photo sequences more than 30 minutes from the next detection of the same species to be independent.

205

206 *Telemetry dataset*

207 We captured and GPS-collared each of the four carnivore species as part of concurrent
208 research on predator-prey relationships. Coyotes were captured in Starkey using padded foothold
209 traps (Oneida Victor SoftCatch No. 3, Euclid, OH) with a tranquilizer tab (Balser 1965)
210 containing 50 mg proprioprom azine hydrochloride attached to each trap to subdue captured
211 animals until researchers arrived. Captured animals were immobilized with tiletamine-zolazepam
212 (Telazol®) at a concentration of 10 mg/kg. A GPS collar (Lotek MiniTrack, Lotek Wireless Inc.,
213 Newmarket, ON, Canada or Vectronic Vertex, Vectronic Aerospace GmbH, Berlin, Germany)
214 was placed on each adult coyote and was programmed to record locations every 2 or 3 hours.
215 We captured bobcats in Starkey using cage traps baited with visual and olfactory
216 attractants or incidentally in foothold traps intended for coyotes. Captured bobcats were
217 administered ketamine (10 mg/kg) and xylazine (1.5 mg/kg) for immobilization, and upon
218 release, yohimbine (0.125 mg/kg; Yobine®) was given as an antagonist for xylazine. Each
219 bobcat was fit with a GPS collar (Lotek MiniTrack, Lotek Wireless Inc., Newmarket, ON,
220 Canada) scheduled to take fixes every 2 hours.
221 Black bears were captured within Starkey using culvert traps or padded foot snares
222 (Lemieux and Czetwertynski 2006). Captured bears were immobilized with Telazol® at a
223 concentration of 7 mg/kg. Bears were fit with GPS collars (Lotek GPS 7000 or LiteTrack Iridium
224 420, Lotek Wireless Inc., Newmarket, ON, Canada) that recorded positions every 15 min to 2
225 hours.
226 We captured cougars using trained pursuit hounds. We searched for fresh cougar tracks in
227 snow and when located, released hounds to pursue tracks until the cougar was treed. Our search

area consisted of Starkey plus a buffer of approximately 20 km. Roads within this buffer were searched as randomly as possible and dogs were allowed to pursue tracks of any individual. When treed, cougars were immobilized with ketamine (10 mg/kg) and xylazine (2 mg/kg) via dart gun, and before release administered yohimbine (0.125 mg/kg; Yobine®) as an antagonist for xylazine. A GPS collar (Lotek GPS 4400S, IridiumTrack M, Lotek Wireless Inc., Newmarket, ON, Canada or Vectronic Vertex Lite, Vectronic Aerospace GmbH, Berlin, Germany) was placed on each cougar and was programmed to record locations every 3 hours.

We permanently marked the belting of GPS collars with unique numbers used to identify individuals on camera (Fig. 2d). When possible (i.e. for the larger collars), we also affixed sections of colored heat-shrink plastic tubing over the collar belting to assist with identification (Fig 2a). We also ear tagged each captured animal such that females received ear tags on the left ear and males on the right ear which allowed an additional cue when identifying GPS-collared animals on camera.

We collected biological samples from each captured individual to match the genotypes of GPS-collared animals with genotypes detected by scat detection dogs. For each animal we sampled some combination of tissue, hair, and feces (see Eriksson et al. 2020 for additional details). All animal handling was performed in accordance with protocols approved by the USDA Forest Service, Starkey Experimental Forest Institutional Animal Care and Use Committee (IACUC No. 92-F-0004; protocol #STKY-16-01) and followed the guidelines of the American Society of Mammalogists for the use of wild mammals in research (Sikes 2016).

Modelling Approach

Our approach was to fit a suite of spatially-explicit models across a spectrum of data resolutions (Table 1, Fig. 3) for each species to evaluate the value of each data source and to test whether incorporating additional data improved precision. Each model considered here is a variation of a conventional SCR model (Royle and Young 2008) in which the detection probability $p_{i,j}$ (or rate $\lambda_{i,j}$) decays as a function of the Euclidean distance between the detector *j* and the activity center *s* for individual *i*, $d_{i,j}$, to yield

$$p_{i,j} = p0_{i,j} \times exp(-d_{i,j}/2\sigma^2), \quad (1)$$

where $p0_{i,j}$ is the baseline detection probability when the detector is located exactly at the activity center of the home range, and σ is a spatial scale parameter related to home range size that determines the rate at which detection probability declines with distance from the activity center. The location of each activity center is latent but estimated as the centroid (spatial average) of the detections for each individual.

The observed encounter histories $y_{i,j}$ can be modeled as either a binomial or Poisson random variable, depending on whether the detection process yields binary or count outcomes,

$$y_{i,j} \sim binomial(p_{i,j} \times z_i, K) \text{ or } y_{i,j} \sim Poisson(\lambda_{i,j} \times z_i \times K), \quad (2)$$

where *K* is the number of sampling occasions, and z_i is the data augmentation parameter that can take the values of 0 or 1 (see below). Data augmentation is used to estimate the number of animals in the state space, *S* (an area prescribed to be sufficiently large such that animals with activity centers at the outermost regions of this area have a negligible probability of being detected). z_i determines whether each hypothetical individual in the augmented population is real or not and is governed by a Bernoulli distribution,

$$z_i \sim Bernoulli(\varphi), \quad (3)$$

in which φ is the expected number of activity centers divided by the augmented population size, *M*, described above. The estimated population size *N* (i.e. the number of activity centers in the state space) is then determined by summing over all z_i,

$$N = \sum_{i=1}^{M} z_i, \quad (4)$$

and density *D* is obtained by dividing the population size by the area of the state space, *S*,

$$D = N/S. \quad (5)$$

We assumed a homogenous point process for the distribution of activity centers (*s*) such that the *x* and *y* dimensions of each activity center were uniformly distributed within the defined limits of the state space:

$$s_{i,x} \sim uniform(S_{x,min,}\, S_{x,max}) \quad (6)$$

$$s_{i,y} \sim uniform(S_{y,min,}\, S_{y,max}) \quad (7)$$

Each model subsequently described is based on the same framework as the conventional SCR described above but involves variations due to different data sources or resolutions which are described next.

Spatial Count or 'unmarked SCR'

The spatial count model (Chandler and Royle 2013) does not require individual recognition, so the encounter history $y_{i,j}$ is replaced by a vector of counts of unmarked individuals at each detector (n_j) and encounter rate λ replaces *p*. The counts are now modeled as a Poisson random variable,

$$n_j \sim Poisson(\Lambda_j \times z_i \times K) \quad (8)$$

where

$$\Lambda_j = \lambda 0_{i,j} \sum_{i=1}^{N} exp(-d_{i,j}/2\sigma^2). \quad (9)$$

295

296 *Spatial Mark-Resight*

297 Spatial mark-resight models (Chandler and Royle 2013, Sollmann et al. 2013a) combine
298 SCR and SC. Here, a subset of the population is individually recognizable due to either natural or
299 artificial markings but the remaining individuals are observed without individual identity. The
300 Poisson distributed encounter history $y.marked_{i,j}$

301 $$y.marked_{i,j} \sim Poisson(\lambda.resight_{i,j} \times z_i \times K) \quad (10)$$

302 is obtained for marked individuals and the resulting expected resighting rate $\lambda.resight_{i,j}$

303 $$\lambda.resight_{i,j} = \lambda 0.resight_{i,j} \times exp(-d_{i,j}/2\sigma^2) \quad (11)$$

304 is applied to the counts of unmarked individuals n_j by replacing $\lambda 0_{i,j}$ in Eq. 9 with
305 $\lambda 0.resight_{i,j}$. An assumption of this model is therefore that marked and unmarked individuals
306 have the same rate of detection.

307

308 *Generalized Spatial Mark-Resight*

309 Generalized spatial mark-resight (gSMR; Whittington et al. 2018) is identical to the
310 conventional SMR described above but incorporates a submodel for the marking (i.e. physical
311 capture and tagging) process and is therefore suitable only when a portion of the population is
312 captured and marked. Generalized SMR alleviates bias introduced due to heterogeneity of
313 individual encounter rate arising from situations when the marked portion of the population
314 resides nearer to the resighting detectors (and are therefore detected more frequently) than
315 unmarked individuals at the periphery of the state space (Whittington et al. 2018). That is, it
316 accounts for the fact that the marked segment of the population is seldom distributed randomly

317 throughout the state space (Whittington et al. 2018). The marking process submodel is itself a
318 SCR model for the encounter histories of individuals captured and marked, $y.marking_{i,j}$,

319 $$y.marking_{i,j} \sim binomial(p.marking_{i,j} \times z_i, K) \quad (12)$$

320 where the probability of capturing individual *i* in trap *j* similarly decays with distance according
321 to

322 $$p.marking_{i,j} = p0.marking_{i,j} \times exp(-d_{i,j}/2\sigma^2). \quad (13)$$

323 The animal capture and marking process and the resighting of marked animals on cameras
324 (SMR) shares information on z_i, s_i, and possibly σ, which has the potential to increase model
325 performance and precision.

326

327 *Hybrid Spatial Capture Recapture + Generalized Spatial Mark-Resight*

328 In situations in which SCR data are obtained concurrently with a capture and marking
329 effort, and the marked individuals are resighted on an array of detectors (e.g. trail cameras), we
330 propose data from all three processes can be modeled together in a 'hybrid' SCR + gSMR model.
331 This model incorporates equations 1-7, and 10-13. In this data-rich model, the encounter
332 histories from each of the three data sources must be aligned such that each individual known
333 from either the marking/resighting process or scat detection process corresponds to the same
334 individual, *i*. in the combined model. However, not all known individuals are likely to be
335 detected in all data sources. For marked animals which are known to exist because they were
336 physically captured, the possible outcomes of the detection process are 1) detected by neither
337 camera nor genetics, 2) detected by camera only, 3) detected by genetics only, or 4) detected by
338 both camera and genetics. For unmarked animals (i.e. those not physically captured), the possible
339 outcomes of the detection process are 1) detected by neither camera nor genetics, 2) detected by

genetics only (and without a genotype matching any of the marked individuals), 3) detected by camera only without individual identity, and 4) detected by camera and genetics (and without the possibility of deterministically linking the genotype to the photographed individual). Information on z_i, s_i, and σ can be shared, and baseline detection rates can be informed by the different data sources when an individual is detected by one but not all detection methods. For example, knowing a captured animal exists but was not detected by genetics can help inform the probability of detection in the genetic SCR component. Similarly, knowing a captured animal exists but was not photographed informs the detection probability for the SMR model component.

Incorporating telemetry data

If some animals within the population are fit with GPS collars (or other telemetry method) during the time sampling is conducted, the telemetry positions can be incorporated into any of the models previously described (Royle et al. 2013, Sollmann et al. 2013a). This is achieved by modelling both the easting and northing GPS positions as a normal distribution centered on the activity center coordinates of individual i, ($s_{i,x}$, $s_{i,y}$), and constraining the variance to be the same in both models, which is equivalent to a bivariate normal distribution with no covariance (Garton et al. 2001):

$$Telemetry, x \sim normal\left(s_{i,x}, \sigma^2\right) \quad (14)$$

$$Telemetry, y \sim normal\left(s_{i,y}, \sigma^2\right) \quad (15)$$

Thus, the incorporation of telemetry data directly informs both the location of the activity center s_i and the scale parameter in the detection function σ. However, in the spatial count models,

362 individual recognition is not known, which prevents the GPS data from being linked to specific
363 individuals, so in those models the telemetry data only inform σ.
364
365 *Application*
366 For each of the four study species (black bear, bobcat, cougar, coyote), SC models were
367 fit using camera data. Individual identity was ignored in SC models even when it was known so
368 that we could evaluate an approach that required no individual recognition. SMR and gSMR
369 models were constructed from the same camera data as the SC models but GPS-collared animals
370 were identified to individual, with the latter method also including the encounter histories from
371 the marking process. SCR models were constructed only from genetic samples (scats) because
372 we could not identify individuals from cameras unless they were artificially marked. The gSMR
373 + SCR hybrid model that we developed combined cameras, physical capture histories, and
374 genetic samples. We assumed that camera and scat data were independent because 1) both data
375 collection methods passively sampled the population in different ways and at different sites
376 within the superpopulation, 2) the detection of a scat did not influence the probability of that
377 individual being detected by camera (and vice-versa), and 3) neither camera placements nor scat
378 dog survey routes were influenced by the knowledge gained from the other method.
379 For every modeling method implemented (Table 1, Fig. 3), we fit models both with and
380 without GPS data. When telemetry data were included, we randomly selected 100 GPS locations
381 (Fig. 2b) to alleviate lack of independence arising from temporal autocorrelation.
382 For the genetic SCR analyses, we used a single occasion because detection dogs only
383 surveyed each gridcell once. We overlaid a 1 x 1 km grid over the survey area and attributed the
384 location of any scat inside that cell to the gridcell center. We modeled the effect of the survey

385 distance of the scat dog route within each gridcell on $p0$ (Eq. 1) using a linear model with a logit
386 link. Samples belonging to the same individual that were found in the same gridcell were
387 recorded as a single detection of individual i. Because some carnivore species defecate
388 nonrandomly as a means of scent marking, we believe removing recaptures within the same
389 gridcell helped ensure independence of samples.

390 For camera analyses, we parsed the encounter data into ten 14-day occasions beginning
391 15 April. We multiplied the detection function by the proportion of the occasion that each
392 camera was operational so that nonfunctioning cameras would not contribute to the model's
393 likelihood. Similarly, if an animal marked at some point during the sampling period was not
394 available to be detected during one or more occasions due to collar loss, death, or because it was
395 not yet collared, we did not allow that individual to contribute to the likelihood for that occasion.

396 We initially sought to include sex-specific detection and scale parameters but abandoned
397 the effort because we had insufficient data on sex for SC and SMR models. Including sex-
398 specific parameters for some but not all models would make meaningful comparisons difficult
399 given our primary interest was to compare inference between model types.

400 To ensure that we included a sufficiently large state space and number of augmented
401 individuals, for each species and model we ensured that M was substantially higher than the
402 estimated N, that the upper bound of φ was not near 1, and that the buffer around the survey area
403 which formed the state space was > 2.5 times σ.

404 To assess and compare dispersion across model types, we calculated the coefficient of
405 variation as the posterior standard deviation divided by the posterior mean. We refer to precision
406 as the inverse of the coefficient of variation rather than the inverse of the variance.
407

Model implementation

We conducted Markov Chain Monte Carlo (MCMC) simulations to estimate the posterior distributions for the parameters of interest in all models. We used JAGS (Plummer 2003) in program R version 3.6.1 (R Development Core Team 2019) and the jagsUI package (Kellner 2015). For each model we ran 3 parallel chains consisting of 10,000 iterations per chain and discarded the first 9,000 as burn in. We assessed model convergence by visually inspecting traceplots and ensuring the $\hat{R}$ values were less than 1.1 (Gelman 1996). If models failed to converge after the first run, we updated them until convergence was satisfactory. For all parameters, we calculated the 95% highest posterior density intervals (HPDI) and 95% Bayesian credible intervals (BCI) (Chen and Shao 1999). For estimates of population size or density, which may be sensitive to the amount of data augmentation prescribed, we report the posterior mode in the text but also present the posterior means and medians in tables.

RESULTS

Our capture efforts yielded GPS collars placed on 6 black bears, 4 bobcats, 6 cougars, and 9 coyotes that were able to be resighted and remained within the bounds of the state space during the time camera and scat sampling occurred. We obtained 124 independent photo sequences for bears (26 marked, 98 unmarked), 34 photo sequences of bobcats (9 marked and 25 unmarked), 48 photo sequences of cougars (24 marked, 24 unmarked), and 479 photo sequences of coyotes (55 marked, 424 unmarked; Table 1). Scat dogs located 86 bear scats, 107 bobcat scats, 18 cougar scats, and 772 coyote scats. Of these, we successfully genotyped 43 bear scats out of 72 attempts (60% success rate), 86 bobcat scats out of 95 attempts (91% success rate), 15 cougar scats out of 17 attempts (88% success rate), and 201 coyote scats out of 216 attempts

(93% success rate). After removing duplicate scats from the same individual in the same gridcell, we had 40 bear scats from 31 individuals, 68 bobcat scats from 32 individuals, 13 cougar scats from 7 individuals, and 165 coyote scats from 83 individuals (Table 1).

All models converged such that $\hat{R}$ was less than 1.1 except for the bobcat SC model not informed by telemetry, which after nearly 30 days of runtime had still not converged. Other SC models without telemetry were slow to converge, exhibited poor mixing of chains, and were possibly unstable.

Telemetry Data

Across all species and methods, the inclusion of GPS data resulted in a mean decrease in the posterior modes for animal densities of 2.4% (Fig. 4, Appendix S3: Tables S1–S4). For all methods except spatial count models, including GPS data led to a mean decrease in the coefficients of variation of 19.9% (Fig. 5, Appendix S3: Tables S1–S4). But in spatial count models, including GPS data increased the coefficients of variation by an average of 144.0% (Fig. 5, Appendix S3: Tables S1–S4). However, very low SC+GPS density estimates were responsible for the increases in the coefficients of variation in those models—standard deviations were actually smaller in SC models including GPS data.

Spatial Capture Recapture

We report SCR+GPS estimates as the benchmark to which the other methods are compared because they are the most data-rich models of the methods tested. The SCR+GPS estimate of the posterior mode (and 95% BCI) for black bears was 9.1/100 km^2 (6.1–18.6 /100 km^2); for bobcats was 12.1/100 km^2 (8.4–16.2/100 km^2), for cougars was 1.7/100 km^2 (0.9–3.6/km^2); and for coyotes was 25.4/100 km^2 (21.0–30.9/100 km^2) (Fig. 4, Appendix S3: Tables S1–S4).

454 *Spatial Count*

455 Spatial count models produced highly divergent results depending on whether telemetry
456 data were included (Fig. 4; Appendix S3: Tables S1–S4). When GPS data were not included,
457 densities from SC models were on average 795.8% higher than SCR+GPS estimates (Fig. 4, Fig.
458 6). However, when GPS data were included, densities from SC models were on average 78.1%
459 lower than SCR+GPS estimates (Fig. 4, Fig. 6). Coefficients of variation for SC and SC+GPS
460 models were 75.1% or 243.1% greater than SCR+GPS, respectively (Fig. 5, Appendix S3:
461 Tables S1–S4).

462 *Spatial Mark-Resight vs Spatial Capture Recapture*

463 On average, SMR+GPS models estimated animal densities that were only 7.3% lower
464 than SCR+GPS models (Fig. 4, Fig. 6, Appendix S3: Table S1–S4). Coefficients of variation
465 were 49.3% higher in SMR+GPS models than SCR+GPS models (Fig. 5, Appendix S3: Tables
466 S1–S4).

467 *Spatial Mark-Resight vs Generalized Spatial Mark-Resight*

468 Across all models and species, adding the marking process to SMR models (i.e. SMR vs
469 gSMR) decreased estimates of animal density by an average of only 0.9% (Fig. 4, Fig. 6,
470 Appendix S3: Tables S1–S4). However, the coefficients of variation were on average 15.3%
471 lower in gSMR models than SMR models (Fig. 5, Appendix S3: Tables S1–S4).

472 *Spatial Capture Recapture vs Hybrid*

473 The Hybrid+GPS models estimated, on average, densities that were only 3.0% lower than
474 SCR+GPS models (Fig. 4, Fig. 6, Appendix S3: Tables S1–S4). The coefficients of variation
475 were 24.8% lower in the Hybrid+GPS model than the SCR+GPS model (Fig. 5, Appendix S3:
476 Tables S1–S4).

DISCUSSION

Many applications in ecology depend on unbiased and precise estimates of animal density. Despite tremendous advancements in wildlife monitoring technology (e.g. remote cameras), molecular methods (e.g. genotyping), and statistics (e.g. models accounting for imperfect detection), estimating population density can still be a formidable task. Biased or imprecise density estimates may at best lead to faulty inference and at worst put populations at risk due to misguided conservation or management efforts. We found that SMR models based on resighting marked animals on cameras produced density estimates consistent with genetic SCR models for bears and cougars, but there was some divergence for bobcats for which the posterior mode of SCR estimates were on average 78.4% higher than the SMR results and for coyotes for which SCR estimates were on average 22.1% lower than the SMR results. For both species, the posterior mode of the SCR models was contained in both the 95% HPDI and BCI of SMR models, but the converse was not true (Fig. 4, Appendix S3: Tables S2 and S4). In contrast, SC models reliant on photos of unmarked animals produced highly divergent density estimates. For all four species, we observed the same pattern in which spatial count models without GPS data exhibited positive bias and spatial count models with GPS data exhibited negative bias compared to models with individual recognition. Informing σ with telemetry data did not lead to accurate enumeration of activity centers and instead falsely attributed unmarked photo detections to too few individuals.

SC models require sufficiently close trap spacing so that spatial autocorrelation can be detected and used to identify activity centers (Chandler and Royle 2013). Poor density estimation from SC models can result from insufficient spatial structure of animal detections that prevent

individual activity centers from being clearly demarcated. However, our 1 km camera grid spacing allowed for many cameras per animal home range, suggesting that these models are not robust for carnivores even with relatively ideal conditions. Further, SC results can be unreliable, unstable, or suffer from convergence failure when data are sparse (Chandler and Royle 2013, Ramsey et al. 2015, Kane et al. 2015, Burgar et al. 2018a, Burgar et al. 2018b, Murphy et al. 2018b), suggesting that this will be a consistent challenge in carnivore studies using unbaited cameras within a time frame over which demographic closure can be reasonably assumed. Recent work has also shown that populations with large values of σ can produce biased results in SC models (Augustine et al. 2019). Including habitat covariates that influence spatial density may in some cases offset bias (e.g. Evans and Rittenhouse 2018), but our results suggest that fully unmarked SCR models (i.e. SC) are often unsuitable for density estimation of the carnivores we studied, particularly when detectors are widely spaced, count data are sparse, and auxiliary data are not available. Given the poor performance of SC models in our analysis, with or without inclusion of telemetry data, we do not recommend this method be used for carnivore species that cannot be uniquely identified in photographs.

Although SMR models and SCR models produced qualitatively similar density estimates, the moderate divergence in results for bobcats and coyotes may be due to challenges when simultaneously camera trapping for multiple species with distinct habitat preferences, home range sizes, and life history strategies. Based on GPS data, bobcats in this system used dense forest cover and our camera placements were biased away from this habitat type because they had extremely limited viewsheds that would limit photos of other species. In contrast, detection dogs readily located bobcat scats and the higher detection probability and sample size of scats may have driven the difference in results between cameras and genetics. Although SCR

523 estimates were 78.4% higher than SMR estimates for bobcats, the discrepancy only amounted to
524 a difference of 5-6 individuals/100 km^2. The disagreement could also be explained if detection
525 dogs found scats from bobcat kittens that were not detected on camera. Because bobcats can give
526 birth nearly year-round (Winegarner and Winegarner 1982), we cannot discount the possibility
527 that kittens were recruited during the time of sampling.

528 For coyotes, the discrepancy between SMR and SCR models may involve unmodeled
529 sources of individual heterogeneity in detection rates across methods as was observed by
530 Murphy et al. (2018a) who estimated lower densities when models were constructed solely from
531 scat data than from both scat and hair. The authors speculated that the behavioral status of
532 coyotes (i.e. resident vs transient) led to cohorts that were disproportionately detected using one
533 detection method over another. Specifically, they reasoned that territorial resident coyotes could
534 be more likely to be detected from scats because of smaller home ranges and increased scent-
535 marking with scat for territorial defense than wide-ranging transients. Our study may exhibit an
536 analogous issue if cameras detected both resident and transient coyotes at high rates but the
537 detected scats disproportionately belonged to residents.

538 Similarly, Morin et al. (2016) suggested that SCR density estimation in coyotes could be
539 improved by modeling heterogeneity in σ and baseline detection rates arising as a result of
540 behavioral status. Without modelling heterogeneity, the bimodality in home range size can lead
541 to estimates of detection and scale parameters that are averaged between the two behavioral
542 states (Murphy et al. 2018). To explore whether failing to acknowledge these sources of
543 heterogeneity were responsible for the divergent results between SMR and SCR models, we
544 conducted a post-hoc analysis where σ and baseline detection parameters were allowed to vary as
545 a function of transient or resident behavioral status (see Appendix S4 for details). Including

546 behavioral status increased the estimates of density in both SMR+GPS and SCR+GPS models
547 but reduced the difference between them from 22% to 16% (Fig. 7). We thus speculate that the
548 unmodeled heterogeneity arising from the distinct behavioral states drove some but not all of the
549 disagreement between model types.

550 Previous studies have successfully estimated population densities of multiple carnivore
551 species using camera trapping (Jiménez et al. 2017, Burgar et al. 2018a, Rich et al. 2019). Our
552 study also suggests a multi-species monitoring approach is possible yet highlights the challenges
553 of simultaneous density estimation of multiple species. For example, the substantial variation in
554 home range size among carnivores requires fine-scale sampling for smaller ranges (e.g. coyotes
555 and bobcats) while allowing for the larger extents needed for greater home range sizes (e.g. bears
556 and cougars). This can be accomplished with either a finely-spaced grid (this study) or through
557 cameras that are clustered with variable spacing intervals (Rich et al. 2019, Murphy et al. 2019).
558 Similarly, assumptions of demographic closure may be challenging to meet for larger home
559 range species unless the extent of the study area is large enough to contain many home ranges.
560 For example, our small survey area relative to the species with the largest home range (e.g. only
561 7 distinct cougars were sampled from genetics) may have made our estimates sensitive to the
562 assumption of demographic closure given that the death, dispersal, or recruitment of even one
563 individual could have a substantial influence on estimates.

564 For all species, the inclusion of telemetry data to inform density estimation generally
565 produced consistent results with increased precision and smaller coefficients of variation for all
566 methods except spatial count models (Fig. 5, Appendix S3: Tables S1–S4). The gains in
567 precision were greatest for the models/species with the sparsest data (e.g. cougar SCR model).
568 Inclusion of GPS data for coyotes increased precision but led to consistently lower density

569 estimates across methods because 3 nonresident transient coyotes with very large territories
570 inflated estimates of σ, which in turn reduced density estimates. This highlights the challenge of
571 estimating σ when telemetry data are excluded and spatial recaptures are sparse. For example,
572 transient individuals with large home ranges may rarely or never be recaptured, which would
573 falsely suggest low detectability rather than the large value for σ that is evident from telemetry
574 data. The absence of telemetry data can thus lead to both imprecise and biased estimates of σ
575 with consequent effects on other model parameters (i.e. $\lambda 0$ or $p 0$ and N) (Whittington et al.
576 2018). Improving the estimate of σ by incorporating telemetry data should aid in identifiability
577 of other parameters and lead to greater accuracy in the models incorporating GPS data. SC
578 models were particularly problematic because they produced biologically unrealistic density
579 estimates that changed from very high to very low with the inclusion of telemetry data. Although
580 telemetry data decreased precision in SC models, the large reduction in the density estimate
581 when including telemetry data led to an increase in the coefficient of variation because the
582 denominator became smaller. A highly biased result with high precision or low CV invites the
583 possibility of overconfidence in an incorrect result when using SC models.

584 Models that included more information on individual identity had more precise density
585 estimates (Fig. 5), except when the number of genotyped scats was very low. In particular, the
586 small sample of cougar scats led to SCR models that were substantially less precise than SMR
587 models (Fig. 5, Appendix S3: Table S4). For all species, the hybrid model containing camera,
588 physical capture (gSMR), and genetic (SCR) data had the lowest coefficients of variation (Fig. 5)
589 highlighting the benefit of leveraging multiple datasets even if some are sparse.

590 A recent movement in ecological modeling of demographic rates has sought to strengthen
591 inference by leveraging multiple data sources (e.g. Besbeas et al. 2002, Schaub et al. 2007). The

592 data required for SMR and SCR models require a substantial investment of time and money and
593 typically result in sparse data. Integrating multiple sparse data sources is thus an efficient use of
594 resources in addition to the benefits of improving precision and reducing bias. Others have
595 integrated camera and genetic data for spatially-explicit density estimation (Sollmann et al.
596 2013b, Clare et al. 2017, Gopalaswamy et al. 2012), but to our knowledge this has only occurred
597 when animals on camera could always be identified to individual, so the result was a SCR model
598 composed of two different data sources. This contrasts with our approach of combining SMR for
599 a partially-marked population (i.e. those in which not all individuals can be uniquely identified)
600 with genetic SCR data in which every sample was identifiable to individual.

601 Ancillary data associated with genetic or mark-resight data may motivate the decision to
602 collect one data type over another. For example, telemetry data obtained in conjunction with a
603 mark-resight study may be useful not only to inform σ and s_i, but also to classify an animal into a
604 behavioral state such as resident vs transient or breeder vs nonbreeder, and these distinctions
605 may explain important sources of individual heterogeneity in detection rate. The photographs in
606 a mark-resight analysis may also permit identification of juveniles which can easily be censored
607 if the researcher desires to estimate the density of the adult population segment only. While
608 genetic sampling is unlikely to yield these sources of information, it offers other benefits such as
609 the ability to study diet (e.g. Kartzinel et al. 2015), hormone levels (e.g. Gobush et al. 2014), and
610 population structure or genetic diversity (e.g. Goosens et al. 2005), which if useful for other
611 objectives may steer researchers toward that method of data collection. Genetic samples also
612 readily yield the sex of the individual which may not be possible from camera trapping for
613 species that are not sexually dimorphic. The cost of each data collection method may also play a
614 factor in the decision. While both genetics and mark-resight studies may be expensive, when a

segment of the population is already being monitored via telemetry devices, the extra cost to resight marked individuals using cameras may be minimal compared to the cost of a separate genetics SCR study (Whittington et al. 2018). However, in the absence of an existing effort to obtain telemetry data, genetic SCR methods are substantially more cost effective given the expense associated with capturing, collaring, and resighting animals.

We could likely refine our results by modeling species-specific sources of individual heterogeneity as for coyotes (Fig. 7). For example, density estimates for species with disparate home ranges sizes between sexes may improve by incorporating sex-specific detection and spatial scale parameters (Sollmann et al. 2011). We chose not to, however, because information on sex was not available for spatial count models and was only partially observable for mark-resight methods (i.e. for the marked animals only) because the sexes of our study species could not accurately be determined from photos alone. Our approach was to standardize models as much as possible across species for the purpose of comparing data sources and model formulations and this precluded us from considering species-specific nuances beyond the illustrative example for resident and transient coyotes (Fig. 7).

Another extension to our efforts might implement spatial partial identity models to extract even more information from the existing datasets (Augustine et al. 2018). This would allow partial genotypes (Augustine et al. 2019) or photos in which the marked status or individual identity (Augustine et al. 2018, Jiménez et al. 2019) cannot be ascertained to be included in SCR estimation. However, this model extension would minimally influence our results because of the high genotyping success from scats using genotyping by amplicon sequencing (Eriksson et al. 2020) and our relatively high success in identifying marked status or individual identity in our camera trap photos.

638 Knowing how much and what type of data to collect is a challenge confronted by most
639 researchers aiming to efficiently estimate population densities. Our results from a suite of
640 spatially-explicit models for bears, bobcats, cougars and coyotes in a natural system highlight the
641 relative performances of models within the spatial capture recapture family constructed from
642 data of varying sources and resolutions. We acknowledge that in some instances, absolute
643 population densities may not be essential and simply being able to accurately characterize
644 relative changes in trends may be adequate. This may be the case for setting management
645 objectives for common species. In other cases, such as the calculation of extinction risk for
646 imperiled species, getting the most accurate estimates of population size is crucial. We found that
647 the most common method for estimating population size of terrestrial carnivores in the past five
648 years was (spatial) capture recapture and that only a minority of studies used methods that do not
649 require individual recognition (Appendix S1: Fig. 1). This suggests that in most cases,
650 researchers are willing to spend the resources necessary to achieve robust results. Regardless, the
651 method chosen must be commensurate with the objective of the study.
652 We conclude by suggesting that future research employing SCR or its variants to estimate
653 the density of carnivores (1) not use SC models, (2) use consistent methods among years because
654 variation in density estimates between SMR and SCR could be misinterpreted as population
655 change, (3) incorporate GPS data when possible, and (4) consider combining multiple data
656 sources using the hybrid SMR+SCR model presented here. We note that SCR models with few
657 scats produced density estimates consistent with, but less precise than, a years-long effort to
658 capture carnivores and resight them on camera traps. Given the inadequacy of SC models and
659 expense associated with capturing carnivores to mark them for resighting, we recommend that
660 new studies to estimate population density of carnivores (that are not distinguishable with natural

661 markings) first consider using genetic SCR. The efficacy to do so will continue to increase as
662 noninvasive genetic sampling transitions toward low-cost and high-success genotyping of SNPs
663 by high-throughput sequencing (Eriksson et al. 2020). Finally, newer models to estimate density
664 using unmarked animals, such as the time-to-event and space-to-event family of models (Moeller
665 et al. 2018), provide hope for a cost-effective method to estimate population densities for
666 multiple species. These models will require a similar field test to that presented here prior to their
667 integration into large-scale carnivore monitoring programs.
668
669 ACKNOWLEDGMENTS
670 We thank M. Bianco, K. Bowman, C. Brown, L. Carr, L. Chodelski, T. Craddock, E. Crain, C.
671 Eckrich, M. Esquibel, S. Gillman, M. Goldman, A. Hilger, R. Jensen, C. Kidd, M. Olsen, J.
672 Smith, A. Yancey, and J. Yancey for field support. We thank K. Cronin, S. Gillman, M.
673 Goldman, J. Hart, V. Heilman, R. Jensen, J. Neeley, N. Owen, S. Muñoz for photo tagging
674 support. We thank J. Allen for lab work. We thank R. Chandler and B. Augustine for coding
675 assistance. We thank B. Dick, R. Kennedy, and D. Rea and the USDA Forest Service Pacific
676 Northwest Research Station for logistical support. Funding and/or field equipment was provided
677 from Oregon Hunter's Association, Oregon Trapper's Association, Wildlife and Sportfish
678 Restoration Act, Pittman Robertson Act, Oregon Department of Fish and Wildlife, USDA Forest
679 Service, and Oregon State University.
680
681

682 LITERATURE CITED

683 Augustine, B. C., J. A. Royle, M. J. Kelly, C. B. Satter, R. S. Alonso, E. E. Boydston, and K. R.
684 Crooks. 2018. Spatial capture–recapture with partial identity: an application to camera traps. The
685 Annals of Applied Statistics 12:67–95.
686
687 Augustine, B. C., J. A. Royle, S. M. Murphy, R. B. Chandler, J. J. Cox, and M. J. Kelly. 2019.
688 Spatial capture–recapture for categorically marked populations with an application to genetic
689 capture–recapture. Ecosphere 10:e02627.
690
691 Balser, D. S. 1965. Tranquilizer tabs for capturing wild carnivores. The Journal of Wildlife
692 Management 29:438–442.
693
694 Besbeas, P., S. N. Freeman, B. J. T. Morgan, and E. A. Catchpole. 2002. Integrating
695 mark-recapture-recovery and census data to estimate animal abundance and demographic
696 parameters. Biometrics 58:540–547.
697
698 Borchers, D. L., and M. G. Efford. 2008. Spatially explicit maximum likelihood methods for
699 capture–recapture studies. Biometrics 64:377–385.
700
701 Buckland, S. T., D. R. Anderson, K. P. Burnham, and J. L. Laake. 1993. Distance sampling:
702 estimating abundance of biological populations. Oxford University Press, Oxford, UK.
703

704 Burgar, J. M., A. C. Burton, and J. T. Fisher. 2019. The importance of considering multiple
705 interacting species for conservation of species at risk. Conservation Biology 33:709–715.
706
707 Burgar, J. M., F. E. Stewart, J. P. Volpe, J. T. Fisher, A. C. Burton. 2018b. Estimating density for
708 species conservation: Comparing camera trap spatial count models to genetic spatial capture-
709 recapture models. Global Ecology and Conservation 15:e00411.
710
711 Chandler, R. B., and J. A. Royle. 2013. Spatially explicit models for inference about density in
712 unmarked or partially marked populations. The Annals of Applied Statistics 7:936–954.
713
714 Chen, M. H. and Q. M. Shao. 1999. Monte Carlo estimation of Bayesian credible and HPD
715 intervals. Journal of Computational and Graphical Statistics 8:69–92.
716
717 Clare, J., S. T. McKinney, J. E. DePue, and C. S. Loftin. 2017. Pairing field methods to improve
718 inference in wildlife surveys while accommodating detection covariance. Ecological
719 Applications 27:2031–2047.
720
721 Eriksson, C. E., J. Ruprecht, and T. Levi. 2019. More affordable and effective noninvasive SNP
722 genotyping using high-throughput amplicon sequencing. bioRxiv.
723 https://doi.org/10.1101/776492.
724
725 Evans, M. J., and T. A. Rittenhouse. 2018. Evaluating spatially explicit density estimates of
726 unmarked wildlife detected by remote cameras. Journal of Applied Ecology 55:2565–2574.

Gardner, B., J. A. Royle, and M. T. Wegan. 2009. Hierarchical models for estimating density from DNA mark–recapture studies. Ecology 90:1106–1115.

Garton, E. O., M. J. Wisdom, F. A. Leban, and B. K. Johnson. 2001. Experimental design for radiotelemetry studies. Pages 15–42 in J. Millspaugh and J. Marzluff, editors. Radiotelemetry and animal populations. Academic Press, San Diego.

Gelman, A. 1996. Inference and monitoring convergence. Pages 131–143 in W. R. Gilks, S. Richardson and D. J. Spiegelhalter, editors. Markov chain Monte Carlo in practice. Chapman and Hall/CRC, Boca Raton, Florida, USA.

Gobush, K. S., R. K. Booth and S. K. Wasser. 2014. Validation and application of noninvasive glucocorticoid and thyroid hormone measures in free-ranging Hawaiian monk seals. General and Comparative Endocrinology 195:174– 182.

Goossens, B., L. Chikhi, M. F. Jalil, M. Ancrenaz, I. Lackman-Ancrenaz, M. Mohamed, P. Andau, and M. W. Bruford. 2005. Patterns of genetic diversity and migration in increasingly fragmented and declining Orangutan (*Pongo pygmaeus*) populations from Sabah, Malaysia. Molecular Ecology 14:441– 456.

748 Gopalaswamy, A. M., J. A. Royle, M. Delampady, J. D. Nichols, K. U. Karanth, and D. W.
749 Macdonald. 2012. Density estimation in tiger populations: combining information for strong
750 inference. Ecology 93:1741–1751.
751
752 Jiménez, J., J. C. Nuñez-Arjona, C. Rueda, L. M. González, F. García-Domínguez, J. Muñoz-
753 Igualada, and J. V. López-Bao. 2017. Estimating carnivore community structures. Scientific
754 Reports 7:1–10.
755
756 Kane, M. D., D. J. Morin, and M. J. Kelly. 2015. Potential for camera-traps and spatial mark-
757 resight models to improve monitoring of the critically endangered West African lion (*Panthera*
758 *leo*). Biodiversity and Conservation 24:3527–3541.
759
760 Kartzinel, T. R., P. A. Chen, T. C. Coverdale, D. L. Erickson, W. J. Kress, M. L. Kuzmina, D. L.
761 Rubenstein, W. Wang, and R. M. Pringle. 2015. DNA metabarcoding illuminates dietary niche
762 partitioning by African large herbivores. Proceedings of the National Academy of Sciences of
763 the United States of America 112:8019– 8024.
764
765 Kellner, K. F. jagsUI: A wrapper around rjags to streamline JAGS analyses. R package version
766 1.3.1. 2015.
767
768 Kery, M., B. Gardner, T. Stoeckle, D. Weber and J. A. Royle. 2011. Use of spatial
769 capture-recapture modeling and DNA data to estimate densities of elusive animals. Conservation
770 Biology 25:356–364.

Lemieux, R., and S. Czetwertynski. 2006. Tube traps and rubber padded snares for capturing American black bears. Ursus, 17:81–92.

Massey, A. L., G. Roffler, T. Vermeul, J. M. Allen, and T. Levi. 2019. Comparison of mechanical sorting and DNA metabarcoding for diet analysis with degraded wolf scats. bioRxiv. https://doi.org/10.1101/2019.12.13.875898.

McClintock, B. T., and G. C. White. 2009. A less field-intensive robust design for estimating demographic parameters with mark–resight data. Ecology 90:313–320.

Moeller, A. K., P. M. Lukacs, and J. S. Horne. 2018. Three novel methods to estimate abundance of unmarked animals using remote cameras. Ecosphere 9:e02331.

Morin, D. J., M. J. Kelly, and L. P. Waits. 2016. Monitoring coyote population dynamics with fecal DNA and spatial capture–recapture. The Journal of Wildlife Management 80:824–836.

Morin, D. J., L. P. Waits, D. C. McNitt, and M. J. Kelly. 2018. Efficient single-survey estimation of carnivore density using fecal DNA and spatial capture-recapture: a bobcat case study. Population Ecology 60:197–209.

Murphy, M. A., L. P. Waits, and K. C. Kendall. 2000. Quantitative evaluation of fecal drying methods for brown bear DNA analysis. Wildlife Society Bulletin 28:951–957.

Murphy, S. M., B. C. Augustine, J. R. Adams, L. P. Waits, and J. J. Cox. 2018a. Integrating multiple genetic detection methods to estimate population density of social and territorial carnivores. Ecosphere 9:e02479.

Murphy, A., B. D. Gerber, Z. J. Farris, S. Karpanty, F. Ratelolahy, and M. J. Kelly. 2018b. Making the most of sparse data to estimate density of a rare and threatened species: a case study with the fosa, a little-studied Malagasy carnivore. Animal Conservation 21:496–504.

Murphy, S. M., D. T. Wilckens, B. C. Augustine, M. A. Peyton, and G. C. Harper. 2019. Improving estimation of puma (*Puma concolor*) population density: clustered camera-trapping, telemetry data, and generalized spatial mark-resight models. Scientific Reports 9:1–13.

Nichols, J.D. 1992. Capture-recapture models. BioScience 42:94–102.

Niedballa, J., R. Sollmann, A. Courtiol, and A. Wilting. 2016. camtrapR: an R package for efficient camera trap data management. Methods in Ecology and Evolution 7:1457–1462.

Otis, D. L., K. P. Burnham, G. C. White, and D. R. Anderson. 1978. Statistical inference from capture data on closed animal populations. Wildlife Monographs 62:3–135.

815 Plummer, M. 2003. JAGS: a program for analysis of Bayesian graphical models using Gibbs
816 sampling. Proceedings of the 3rd International Workshop on Distributed Statistical Computing
817 (DSC 2003), March 20–22, Vienna, Austria.
818
819 R Development Core Team. 2019. R: A language and environment for statistical computing. R
820 Foundation for Statistical Computing, Vienna, Austria.
821
822 Ramsey, D. S., P. A. Caley, A. Robley. 2015. Estimating population density from presence–
823 absence data using a spatially explicit model. The Journal of Wildlife Management 79:491–499.
824
825 Riaz, T., W. Shehzad, A. Viari, F. Pompanon, P. Taberlet, and E. Coissac. 2011. ecoPrimers:
826 inference of new DNA barcode markers from whole genome sequence analysis. Nucleic Acids
827 Research 39:e145.
828
829 Rich, L. N., D. A. Miller, D. J. Muñoz, H. S. Robinson, J. W. McNutt, and M. J. Kelly. 2019.
830 Sampling design and analytical advances allow for simultaneous density estimation of seven
831 sympatric carnivore species from camera trap data. Biological Conservation 233:12–20.
832
833 Rowcliffe, J. M., J. Field, S. T. Turvey, and C. Carbone. 2008. Estimating animal density using
834 camera traps without the need for individual recognition. Journal of Applied Ecology 45:1228–
835 1236.
836

837 Rowland, M. M., L. D. Bryant, B. K. Johnson, J. H. Noyes, M. J. Wisdom, and J. W. Thomas.
838 1997. The Starkey project: history, facilities, and data collection methods for ungulate research.
839 PNW-GTR-396. USDA Forest Service Pacific Northwest Research Station, Portland, Oregon,
840 USA.
841
842 Royle, J. A. 2004. N-mixture models for estimating population size from spatially replicated
843 counts. Biometrics 60:108–115.
844
845 Royle, J. A., and J. D. Nichols. 2003. Estimating abundance from repeated presence–absence
846 data or point counts. Ecology 84:777–790.
847
848 Royle, J. A., and K. V. Young. 2008. A hierarchical model for spatial capture–recapture data.
849 Ecology 89:2281–2289.
850
851 Royle, J. A., R. B. Chandler, R. Sollmann, and B. Gardner. 2013. Spatial capture-recapture.
852 Academic Press.
853
854 Schaub, M., O. Gimenez, A. Sierro, and R. Arlettaz. 2007. Use of integrated modeling to
855 enhance estimates of population dynamics obtained from limited data. Conservation Biology
856 21:945– 955.
857

858 Sikes, R. S., & Animal Care and Use Committee of the American Society of Mammalogists.
859 2016. 2016 Guidelines of the American Society of Mammalogists for the use of wild mammals
860 in research and education. Journal of Mammalogy 97:663–688.
861
862 Sollmann, R., M. M. Furtado, B. Gardner, H. Hofer, A. T. Jácomo, N. M. Tôrres, and L. Silveira.
863 2011. Improving density estimates for elusive carnivores: accounting for sex-specific detection
864 and movements using spatial capture–recapture models for jaguars in central Brazil. Biological
865 Conservation 144:1017–1024.
866
867 Sollmann, R., B. Gardner, A. W. Parsons, J. J. Stocking, B. T. McClintock, T. R. Simons, K. H.
868 Pollock, and A. F. O'Connell. 2013a. A spatial mark–resight model augmented with telemetry
869 data. Ecology 94:553–559.
870
871 Sollmann, R., N. M. Tôrres, M. M. Furtado, A. T. de Almeida Jácomo, F. Palomares, S. Roques,
872 and L. Silveira. 2013b. Combining camera-trapping and noninvasive genetic data in a spatial
873 capture–recapture framework improves density estimates for the jaguar. Biological Conservation
874 167:242–247.
875
876 Wasser, S. K., B. Davenport, E. R. Ramage, K. E. Hunt, M. Parker, C. Clarke, and G. Stenhouse.
877 2004. Scat detection dogs in wildlife research and management: application to grizzly and black
878 bears in the Yellowhead Ecosystem, Alberta, Canada. Canadian Journal of Zoology 82:475–492.
879

880 Wasser, S. K., J. L. Keim, M. L. Taper, and S. R. Lele. 2011. The influences of wolf predation,
881 habitat loss, and human activity on caribou and moose in the Alberta oil sands. Frontiers in
882 Ecology and the Environment 9:546–551.
883
884 White, G. C. 1996. NOREMARK: population estimation from mark-resighting surveys. Wildlife
885 Society Bulletin 24:50–52.
886
887 Whittington, J., M. Hebblewhite, and R. B. Chandler. 2018. Generalized spatial mark–resight
888 models with an application to grizzly bears. Journal of Applied Ecology 55:157–168.
889
890 Wilson, G. J., and R. J. Delahay. 2001. A review of methods to estimate the abundance of
891 terrestrial carnivores using field signs and observation. Wildlife Research 28:151–164.
892
893 Winegarner, C. E., and M. S. Winegarner. 1982. Reproductive history of a bobcat. Journal of
894 Mammalogy 63:680–682.
895
896 Wisdom, M. J., M. M. Rowland, B. K. Johnson, and B. L. Dick. 2005. Overview of the Starkey
897 Project: mule deer and elk research for management benefits. Pages 17–28 in M. J. Wisdom,
898 editor. The Starkey project: a synthesis of long-term studies of elk and mule deer. Alliance
899 Communications Group, Lawrence, Kansas, USA.
900
901
902

903 TABLE 1: Description of data requirements for each model evaluated. The data collection sources
904 used in this study are given in parentheses. Models are ordered in terms of increasing data
905 requirements. Sample sizes for the number of independent detections for each data collection
906 method are given in the last column, separated by commas, for black bears, bobcats, cougars, and
907 coyotes, respectively. For sample sizes of genetic samples, we provide both number of unique
908 individuals and number of total samples, respectively, separated by a slash. For brevity we only
909 present sample sizes the first time a certain data type is introduced.
910

Model	**Data Inputs**	**Sample size (for bear, bobcat, cougar, coyote)**
Spatial Count	1. Counts of unmarked individuals (cameras)	124, 34, 48, 479
Spatial Mark Resight	1. Encounter history of marked individuals (cameras) 2. Counts of unmarked individuals (cameras)	26, 9, 24, 55 98, 25, 24, 424
Generalized Spatial Mark Resight	1. Encounter history of marked individuals (cameras) 2. Counts of unmarked individuals (cameras) 3. Encounter history of marking process (live traps)	 6, 4, 6, 9
Spatial Capture Recapture	1. Encounter history of genotypes (scat)	31/40, 33/68, 7/13, 83/165
Spatial Capture Recapture + Marking Process	1. Encounter history of genotypes (scat) 2. Encounter history of marking process (live traps)	

Generalized	1. Encounter history of marked individuals (cameras)
Spatial Mark	2. Counts of unmarked individuals (cameras)
Resight +	3. Encounter history of marking process (live traps)
Spatial Capture	4. Encounter history of genotypes (scats)
Recapture	

911

912

FIGURE LEGENDS

FIG. 1: The study area. The black polygon represents the Starkey Experimental Forest and Range boundary, green points are camera locations, and blue lines are scat detection dog survey tracks.

FIG. 2: a) Immobilized coyote fit with GPS collar. Note the colored shrinkwrap around collar banding and unique number aiding in individual identification when photographed on remote cameras. b) GPS collar positions for coyotes (light green), cougars (blue), bobcats (purple), and bears (red) during the time sampling was conducted. The red outline is the Starkey Experimental Forest and Range boundary. c) Scat located by detection dogs subsequently analyzed for species ID and genotyped to determine individual identity. d) A GPS-collared bear detected on remote camera. The number on the collar belting and location of the ear tag permitted individual identification of this animal.

FIG. 3: A schematic diagram describing the data inputs for each model evaluated in this study. We note that without the inclusion of GPS collar data, σ and s are still estimable but lack the resolution provided by including telemetry data.

FIG. 4: Split violin plots displaying posterior distributions for the densities of bears, bobcats, cougars, and coyotes across a suite of modeling methods. Within each panel, models are ordered in terms of increasing data requirements with the most data-hungry models on the right. For each model type, the left (blue) half of the violin excludes GPS telemetry data and the right (tan) half includes GPS data. The white boxes display the 95% highest posterior density interval, and the middle black bar indicates the posterior mode. Densities are presented as number of animals per

100 km^2. Note that the spatial count models for each species required a different y-axis scale than the other model types.

FIG. 5: Coefficients of variation for density estimates for bears, bobcats, cougars, and coyotes (top left, clockwise). For each model type, the left (blue) bar excludes GPS data and the right (tan) bar includes GPS data. The coefficient of variation was calculated as the standard deviation divided by the posterior mean. Note that the sample size for the cougar SCR models was small (n = 13 scats) and likely caused the relative imprecision for those models.

FIG. 6: Percent difference in the posterior mode of animal density compared to the SCR+GPS model for black bears, bobcats, cougars, and coyotes. Note that the spatial count models for each species required a different y-axis scale than the other model types. The dotted red line refers to no difference from the SCR+GPS model; bars above the line indicate positive bias and bars below the line indicate negative bias with respect to the SCR+GPS model.

FIG. 7: Violin plot showing SMR and SCR density estimates for coyotes modeled with and without behavioral status (i.e. resident or transient). The left two violins show estimates from the standard models while the right two display estimates from the model where sigma and detection rates are allowed to vary as a function of behavioral status.

956 **Figure 1**

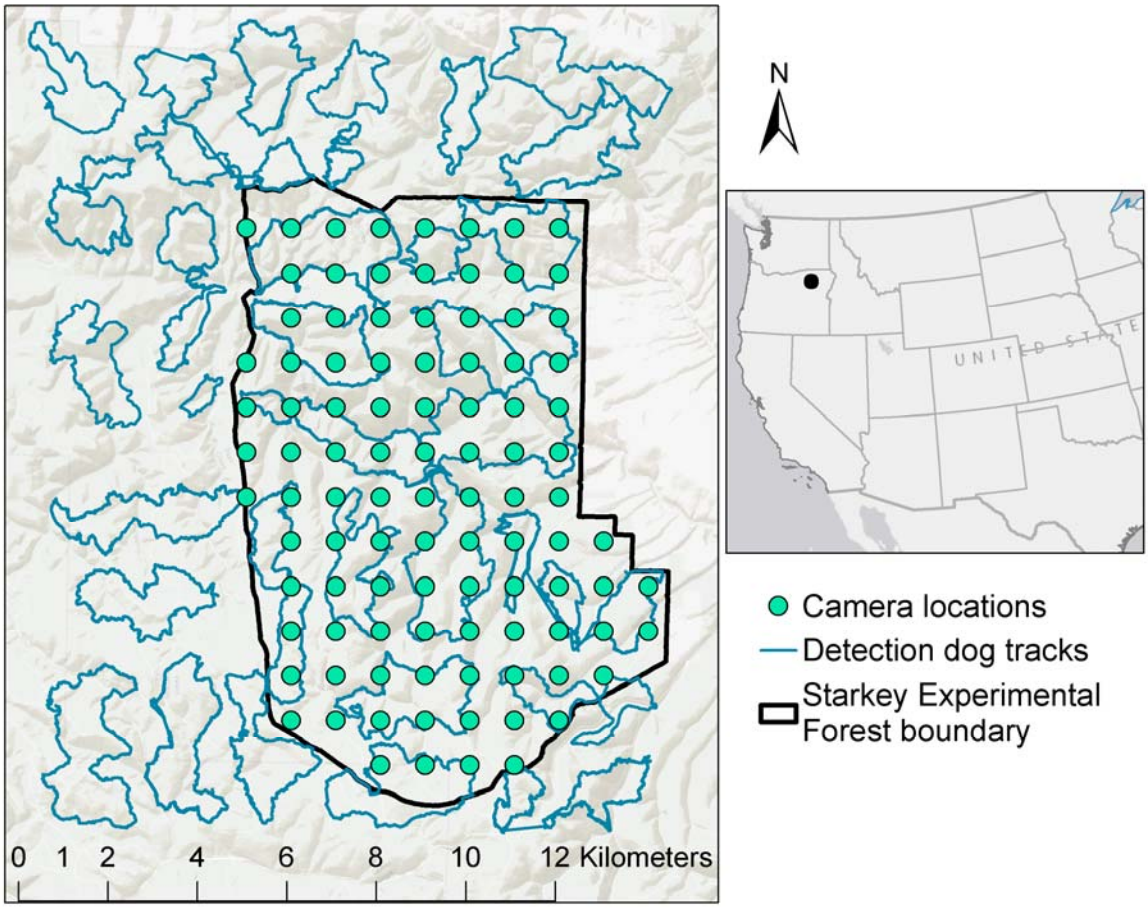

957

958

959

960

961

962

963

964

965

966

967 **Figure 2**

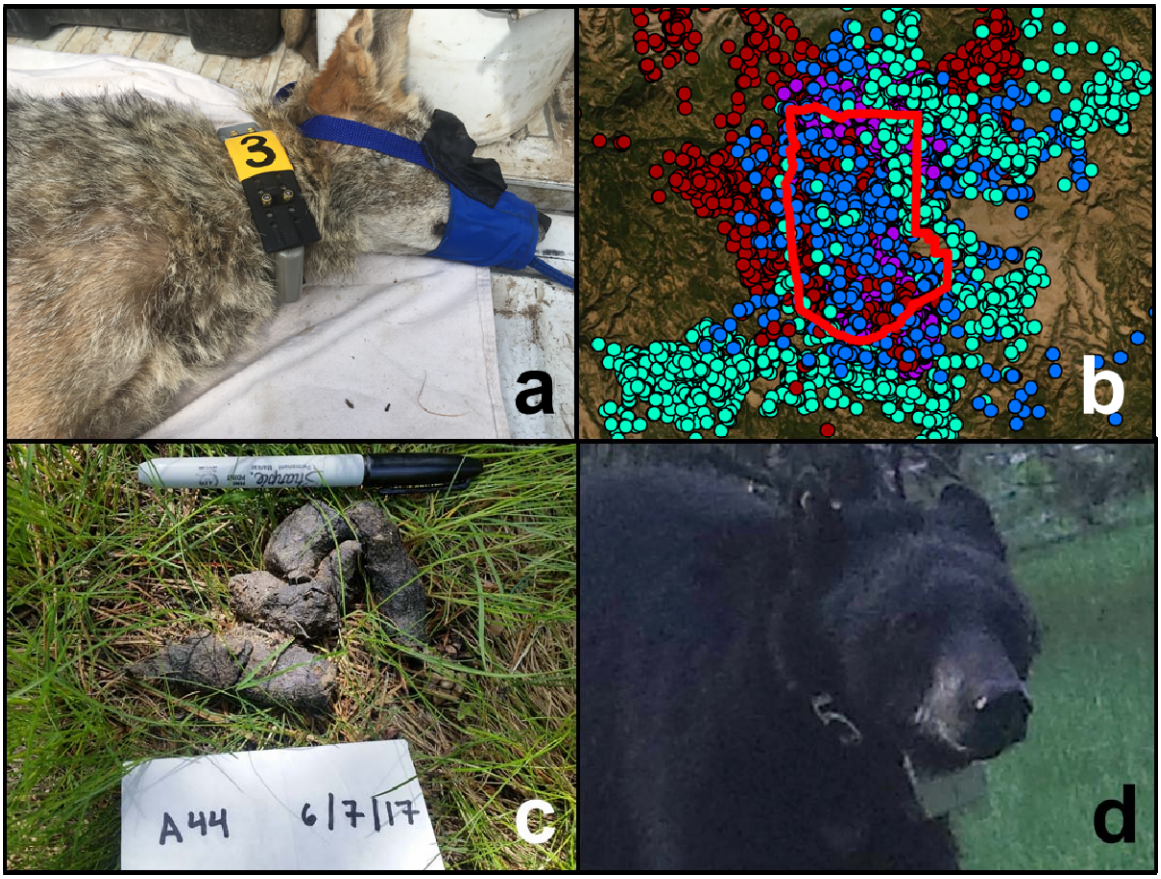

968

969

970

971

972

973

974

975

976

977

978 **Figure 3**

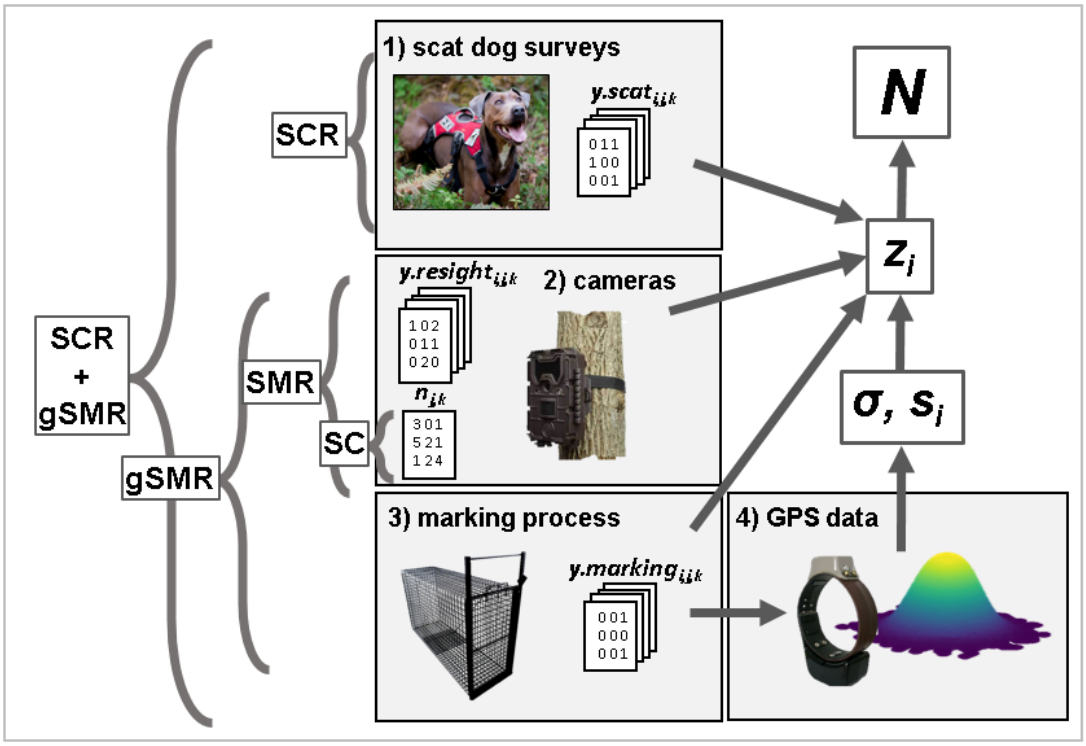

979

980

981

982

983

984

985

986

987

988

989

990

991

992 **Figure 4**

993

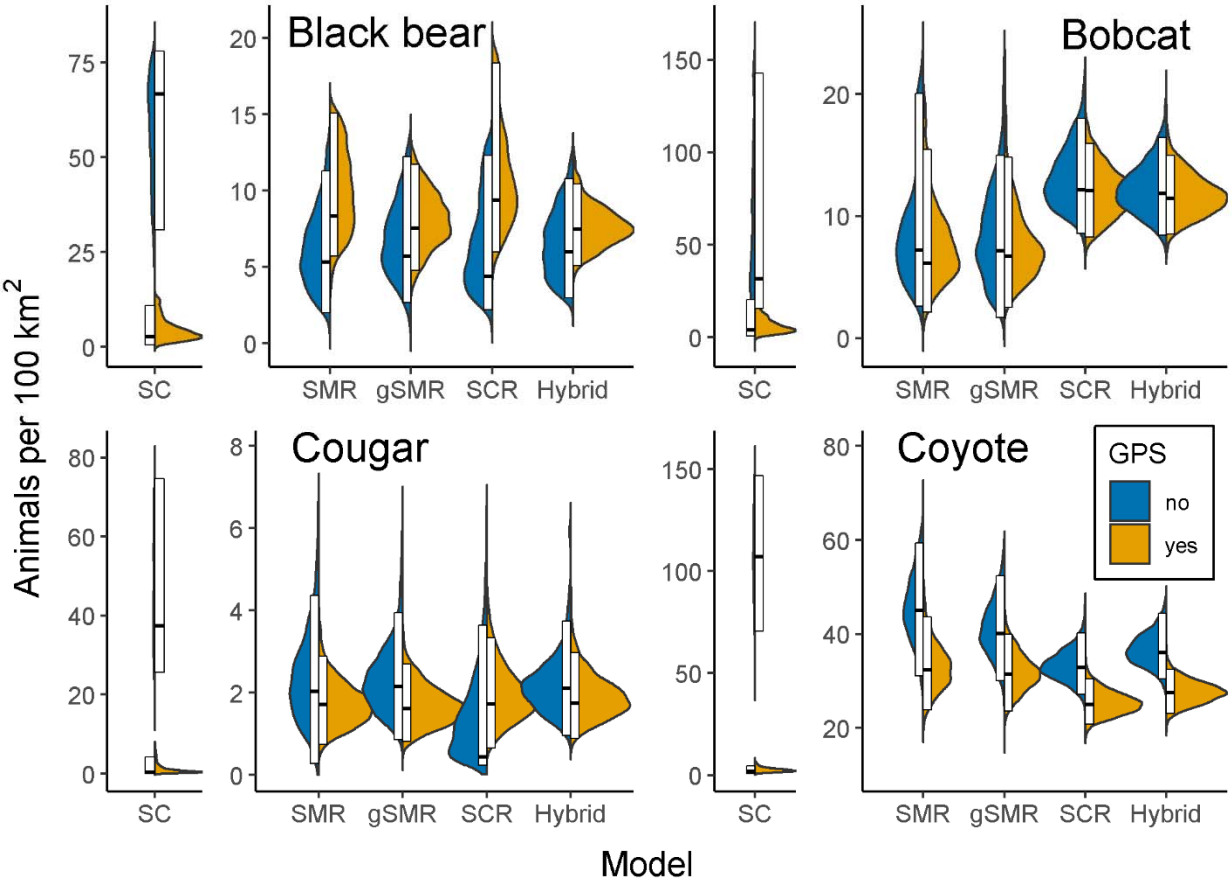

994

995

996

997

998

999

1000

1001

1002

1003

1004 **Figure 5**

1005

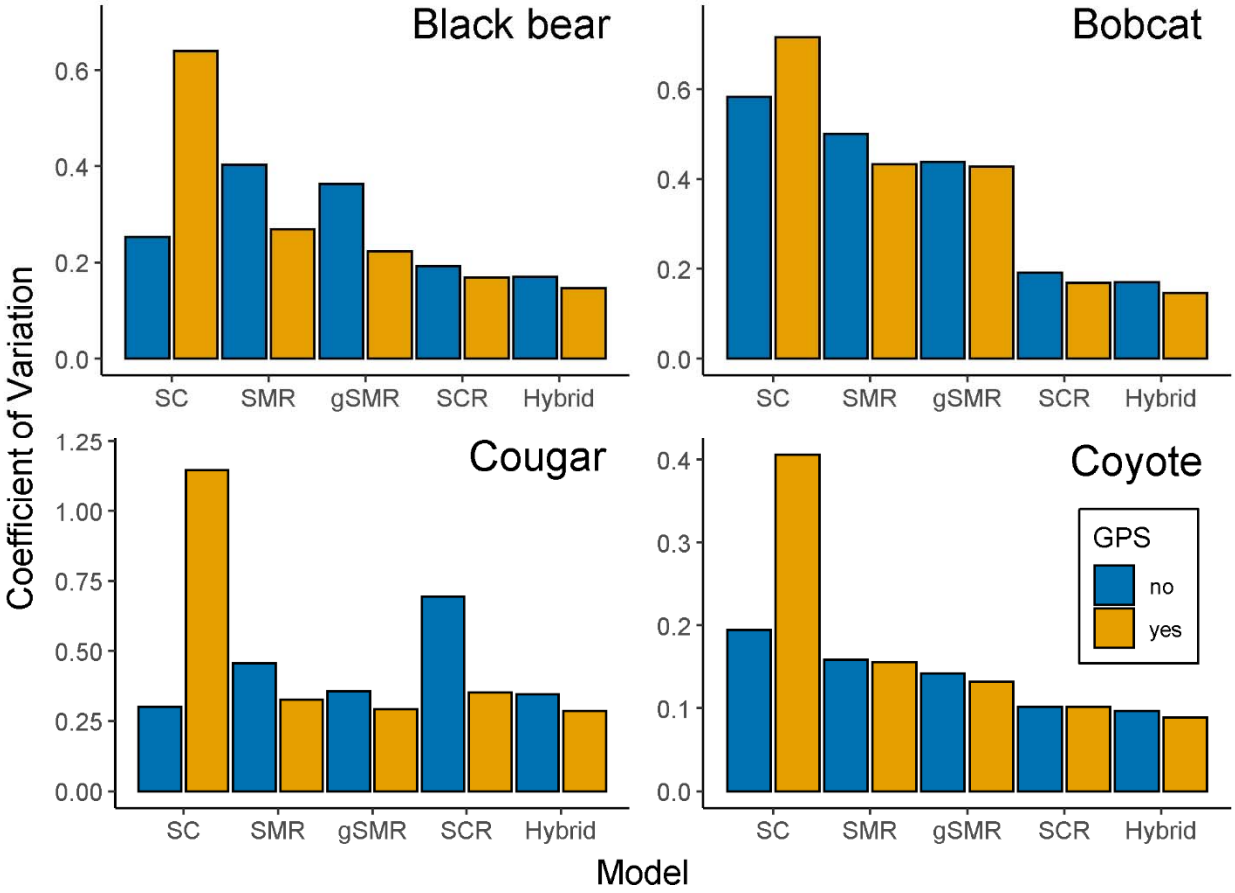

1006

1007

1008

1009

1010

1011

1012

1013

1014

1015 **Figure 6**

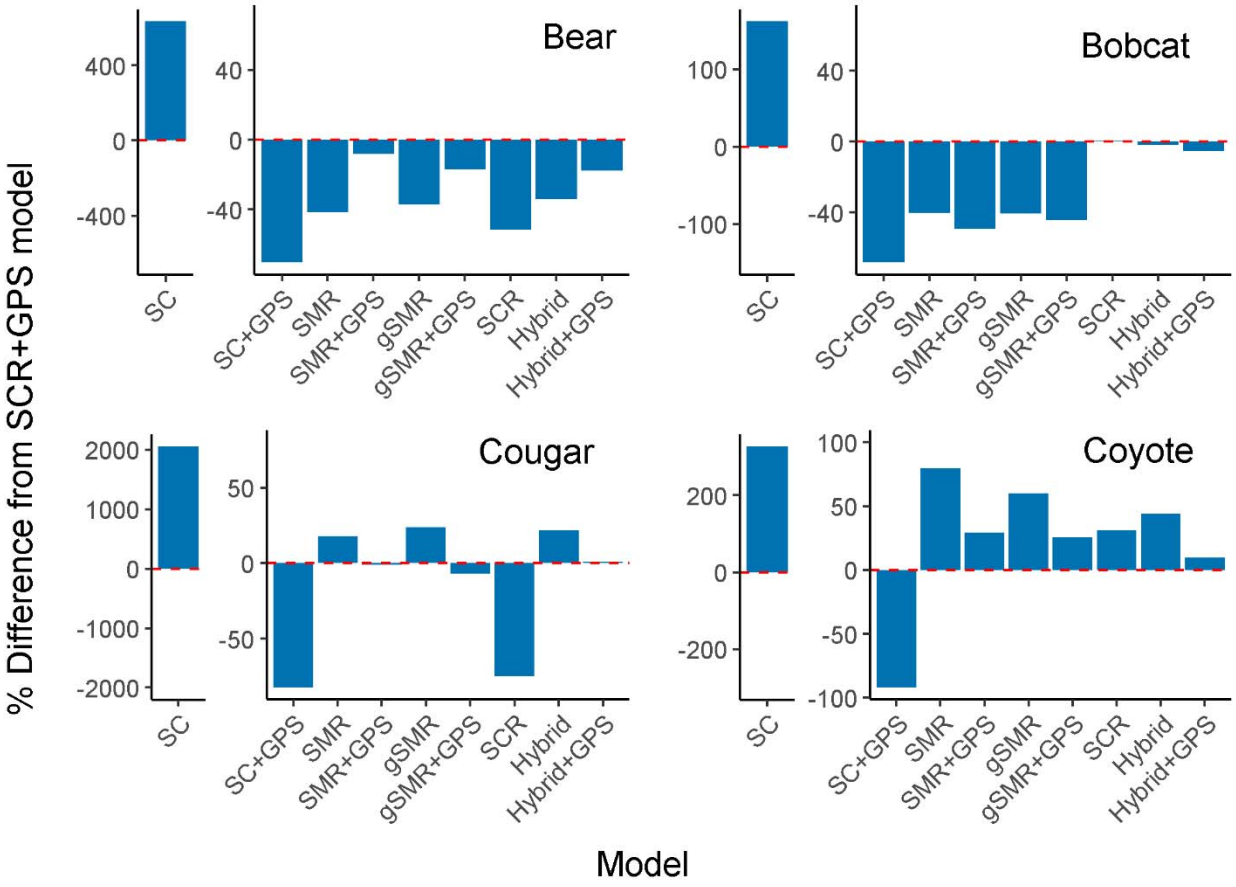

1016

1017

1018

1019

1020

1021

1022

1023

1024

1025 **Figure 7**

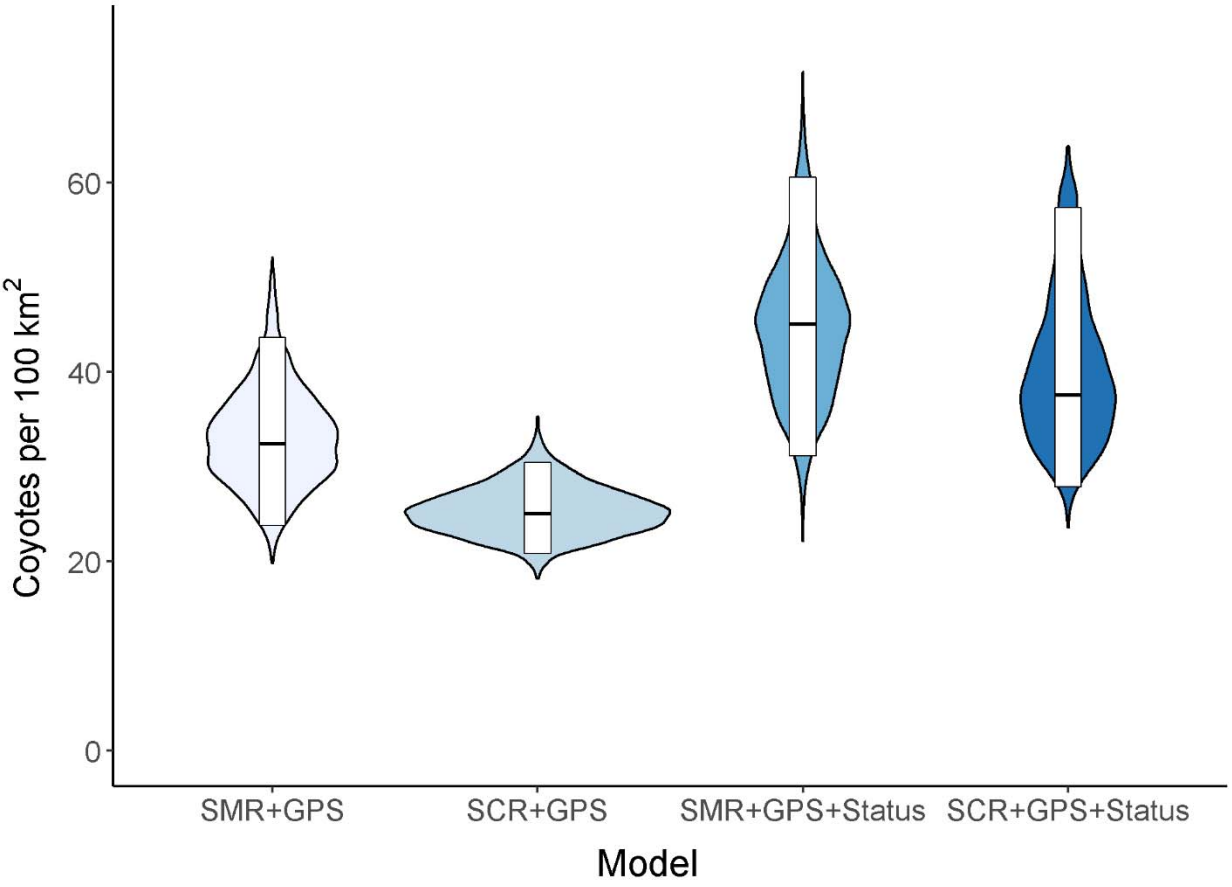

1026

1027

1028

1029

1030

1031

1032

1033

1034

1035